Submitted, accepted and published by
Fuel Processing Technology 124 (2014) 104-114

Biomass combustion with CO_2 capture by Chemical Looping with Oxygen Uncoupling (CLOU)

I. Adánez-Rubio, A. Abad*, P. Gayán, L. F. de Diego, F. García-Labiano, J. Adánez

Instituto de Carboquímica (ICB-CSIC), Miguel Luesma Castán 4, 50018-Zaragoza, Spain

**e-mail: abad@icb.csic.es*

Abstract

Economic benefits can be expected in the future if CO_2 capture and storage is implemented in energy generation from biomass combustion. The aim of this work is to investigate the combustion of biomass in a Chemical Looping with Oxygen Uncoupling (CLOU) process with inherent CO_2 separation. The performance of biomass combustion in a continuously operated 1.5 kW_{th} CLOU unit is presented. Particles prepared by spray drying containing 60 wt.% CuO were used as an oxygen carrier. Milled pine wood chips were used as fuel. The work focused on the effect of fuel reactor temperature on the CO_2 capture and the combustion efficiency of the CLOU process with biomass. Under CLOU operation, biomass combustion was complete to CO_2 and H_2O without the presence of any unburnt material, including tars. Moreover, high carbon capture efficiencies were achieved using very low oxygen carrier inventories and without a carbon separation unit. This is the first time that the CLOU concept has been demonstrated in a continuous CLC unit using biomass as fuel.

Keywords: Carbon capture, combustion, biomass, CLOU, copper, chemical looping.

1. Introduction

According to the IPCC report on the mitigation of climate change [1], in order to stabilize CO_2 concentration in the atmosphere, CO_2 Capture and Storage (CCS) would contribute 15–55% to the cumulative mitigation effort worldwide until 2100. CCS is a process involving the separation of the CO_2 emitted by industry and energy-related sources and its storage for long term isolation from the atmosphere. Chemical Looping Combustion (CLC) has been suggested as being among the best alternatives to reduce the economic cost of CO_2 capture [2] and to reduce the energy penalty in comparison with other CO_2 capture processes [3]. In this process, CO_2 is inherently separated from other combustion products, N_2 and unused O_2, through the use of a solid oxygen carrier; thus no energy is expended for CO_2 separation. The CLC process has been demonstrated for the combustion of gaseous fuels such as natural gas or syngas in 10 to 140 kW_{th} units using oxygen carrier materials based on nickel, copper and iron. Results obtained for CLC with gaseous fuel with different oxygen carriers have been reviewed by Adanez et al. [4] and Lygfelt [5].

The direct use of solid fuels in the CLC concept for energy generation is highly relevant because solid fuels are considerably more abundant and less expensive than natural gas. CLC with solid fuels involves the fuel being physically mixed with the oxygen carrier in the fuel reactor. The *in-situ* gasification of the solid fuel, e.g. coal, biomass or solid wastes, using steam or CO_2 as a gasification agent [6,7] has been proposed as an intermediate step for fuel conversion. This process has been

demonstrated in units of 10 to 100 kW_{th} with coal [8-10]. The main limitation found in solid fuel conversion in *in-situ* gasification chemical looping combustion process (*i*G-CLC) [4] is the slow gasification process [8,11], as well as the incomplete combustion of gases evolved in the fuel reactor [12].

To overcome the low reactivity of the char gasification step in the *i*G-CLC, an alternative process, Chemical Looping with Oxygen Uncoupling (CLOU), was proposed by Mattisson et al. [13]. They made use of the idea first proposed by Lewis and Gilliland [14] to produce CO_2 from solid carbonaceous fuels by using the gaseous oxygen produced by the decomposition of CuO. The CLOU process is based on the strategy of using oxygen carrier materials which release gaseous oxygen and thereby allows the solid fuel to burn with the gas phase oxygen. These materials can be also regenerated at high temperatures.

Fig. 1 shows a schematic diagram of a CLOU system. The fuel conversion in the fuel reactor is produced by different reactions. First the oxygen carrier releases oxygen according to:

$$2\ Me_xO_y \leftrightarrow 2\ Me_xO_{y-1} + O_2 \quad (1)$$

and the solid fuel begins to devolatilize, producing a carbonaceous solid residue (char, mainly composed of carbon and ash) and volatile matter as gaseous product:

$$\text{Solid fuel} \rightarrow \text{Volatile matter} + \text{Char (C)} \quad (2)$$

The volatiles and char are then burnt in a similar way than in the usual combustion process with the gaseous oxygen according to reactions (3) and (4):

$$\text{Volatile matter} + O_2 \rightarrow CO_2 + H_2O \quad (3)$$

$$\text{Char (C)} + O_2 \rightarrow CO_2 + \text{ash} \quad (4)$$

After steam condensation, a pure CO_2 stream is obtained from the fuel reactor. The reduced oxygen carrier is transported to the air reactor, where the oxygen carrier is

regenerated to the initial oxidation stage with the oxygen in air in readiness for use in a new cycle. Ideally, the exit stream of the air reactor will contain only N_2 and unreacted O_2. The heat release over the fuel and air reactors is the same as for conventional combustion. Therefore, the CLOU process has a low energy penalty for CO_2 separation and low CO_2 capture costs are expected.

The slow gasification step for the direct solid fuel experienced in *i*G-CLC is avoided in the CLOU process, which achieves a much faster solids conversion [15]. It was found that the conversion rate for the solid fuel was increased by a factor of 45 for a petroleum coke [13] and by 60 for a bituminous coal [15] in comparison with those measured using an oxygen carrier without the oxygen uncoupling property. Moreover, the combustion of the fuel consumes the oxygen generated by the oxygen carrier and improves the decomposition reaction of the metal oxide particles [16]. As a consequence, solids inventory as low as 50 kg/MW_{th} were estimated by Adánez-Rubio et al. [16]. These solids inventory is much lower than the ones required in the *i*G-CLC system with solid fuels, which is in the range of 1000-2000 kg/MW_{th} for Fe-based oxygen carriers [17-20].

Thus, a special requisite applies to the oxygen carrier to be used in the CLOU process in comparison with oxygen carriers for normal CLC, where the fuel reacts directly with the solid oxygen carrier without any release of gas phase oxygen. Only those metal oxides that have a suitable equilibrium partial pressure of oxygen at temperatures of interest for combustion (800-1200ºC) can be used as oxygen carrier materials in the CLOU process. Moreover, this O_2 release must be reversible in order to oxidize the oxygen carrier in the air reactor and regenerate the material. CuO/Cu_2O, Mn_2O_3/Mn_3O_4 and Co_3O_4/CoO have been identified as redox pairs with the capacity to

evolve oxygen at high temperature [13]. To date, there are only a small number of developed materials that are suitable for the CLOU process [4, 21-24]

The ICB-CSIC research group performed a screening study that considered 25 different Cu-based oxygen carriers in order to select appropriate materials for the CLOU process [21]. Two promising Cu-based oxygen carriers prepared by pelletizing under pressure (60 wt.% CuO supported on $MgAl_2O_4$, and 40 wt.% CuO supported on ZrO_2) were selected owing to their high reactivity, low attrition rate and lack of agglomeration. After the screening tests, a batch of 60 wt.% CuO supported on $MgAl_2O_4$ was prepared by spray drying and evaluated in a CLOU unit [25]. The validity of the concept of the CLOU process with coal was demonstrated using this material as the oxygen carrier [15] in a 1.5 kW_{th} continuously operated unit consisting of two interconnected fluidized-bed reactors. The effect of the coal rank was also analysed [26] in this unit using a lignite, two bituminous coals and an anthracite. Complete combustion was achieved using a solids inventory in the fuel reactor of 235 kg/MW_{th}. In conjunction, values close to 100 % in carbon capture efficiency were obtained at 960ºC with reactive coals. However, for low reactivity coals such as anthracite, a carbon separation system would be needed in the system to prevent carbon intrusion into the air reactor. Recently, the fate of sulphur in the CLOU process using a Cu-based oxygen carrier was studied in this plant [27] using a high sulphur content fuel. Most of the sulphur introduced with the fuel exited as SO_2 at the fuel reactor outlet and the oxygen carrier particles showed good behaviour as reactivity was unaffected and agglomeration problems did not occur.

If a CO_2 capture system is implemented in a biomass combustion process, the global carbon balance in the atmosphere will be negative, because the carbon dioxide generated was previously removed from the atmosphere by the biomass. Consequently,

biomass is an interesting fuel for testing in CLC or CLOU processes, because it would be possible to obtain negative CO_2 emissions. Only a few studies using biomass as fuel in continuous CLC units [28-30] can be found in the literature. In these studies, the biomass was converted through *in-situ* gasification in the fuel reactor of a CLC system (*i*G-CLC). Iron oxide was used as the oxygen carrier in units of 10 kW_{th} [30] and 1 kW_{th} with a spouted-bed reactor as fuel reactor [28]. There was found to be a high char conversion in the fuel reactor owing to the high reactivity of the biomass char. At the same time, the outlet gases from the fuel reactor had a relevant fraction of unburnt compounds resulting from the large amount of volatiles. Finally, our research group at ICB-CSIC [29] studied the effect of the fuel reactor temperature, solids circulation rate and gasifying agent on the combustion efficiency of milled pine wood chips using iron ore as the oxygen carrier in a continuous 500 W_{th} CLC plant. Carbon capture efficiencies higher than 95% in a temperature range of 880-915ºC were obtained in this study, although combustion efficiency was in the 85-95% range.

Although, the benefits of the CLOU process have been shown in comparison with the *i*G-CLC process [15], to date there have been no studies on the combustion of biomass by the CLOU process in the literature. The aim of this work was therefore to investigate the validity of the concept of the CLOU process in a continuously operated CLOU plant using biomass as fuel. In this work, particles prepared by spray drying containing 60 wt% CuO and using $MgAl_2O_4$ as supporting material were used as the oxygen carrier for the CLOU process. Biomass has higher volatile matter content than coal and different behaviour could be expected during combustion. The effect of fuel reactor temperature on combustion and CO_2 capture efficiencies was investigated.

2. Experimental section

2.1. The Cu-based oxygen carrier

The oxygen carrier used in this work was a Cu-based material prepared by spray drying. The oxygen carrier particles were manufactured by VITO (Flemish Institute for Technological Research, Belgium) using CuO (Panreac, PRS) and $MgAl_2O_4$ spinel (Baikowski, S30CR) as raw materials. The particles were calcined for 24 h at 1100ºC. The CuO content was 60 wt.%. The particle size of the oxygen carrier was +0.1-0.25 mm. From this point on, the oxygen carrier is referred to as Cu60MgAl. Table 1 shows the main properties of this material.

Physical and chemical characterization was carried out with these particles, as shown in Table 1. The copper content was determined by complete reduction in TGA using 15 vol.% H_2 at 850ºC [25]. The oxygen transport capacity, R_{OC}, was calculated in TGA in nitrogen atmosphere at 1000ºC as $R_{OC} = (m_{ox}-m_{red})/m_{ox}$, where m_{ox} is the mass of fully oxidized particles and m_{red} the reduced form after oxygen uncoupling, i.e. once all the CuO is reduced to Cu_2O [25]. Table 1 also shows the different equipment used to characterize this material.

The preliminary results showed that this material had adequate reactivity values and oxygen transport capacity in fluidized-bed conditions [16, 25]. High combustion rates with complete combustion to CO_2 and H_2O were obtained with this material using a low solids inventory in the fuel reactor of a CLOU unit burning different types of coal [15, 26].

2.2. Biomass

Milled pine wood chips from Spain were used for the CLOU experiments with Cu60AlMg. The main properties of this biomass are shown in Table 2. The biomass

particle size used for this study was +0.5-2 mm. This fuel is characterized by its high volatile matter content (81 wt.%) with respect to coal.

2.3. ICB-CSIC-s1 unit for the CLOU process

A schematic view of the experimental set-up used is shown in Fig. 2. The set-up was basically composed of two interconnected fluidized-bed reactors –the air and fuel reactors– joined by a loop seal in the lower and a riser for solids transport from the air reactor to the fuel reactor. A cyclone recovered the solids entrained from the riser. A solids valve controlled the solids circulation flow rate in the system. The reactors operated at slightly higher than atmospheric pressure, taking into consideration the pressure drops in the beds and pipes to the stack. The fuel reactor (1 in Fig.2) consisted of a bubbling fluidized bed with a 50 mm inner diameter and 200 mm bed height. N_2 was used as fluidizing gas instead of CO_2 in order to improve the accuracy for calculation of the carbon burnt in the fuel reactor. In a previous work, it had been determined that the fluidization agent did not have any influence on the oxygen carrier behaviour [21]. The gas flow was 250 L_N/h, corresponding to a gas velocity of 0.15 m/s at 900ºC. The minimum fluidizing velocities of the oxygen carrier particles were 0.006 m/s for the smallest particle size and 0.023 m/s for the biggest, while the terminal velocities of particles were 0.40 m/s and 1.45 m/s respectively.

Fuel (9 in Fig.2) was fed in by a screw feeder (10 in Fig.2) at the bottom of the bed just above the fuel reactor distributor plate in order to maximize the time that the fuel and volatile matter were in contact with the bed material. The screw feeder consisted of two steps: the first with variable speed to control the fuel flow rate; the second was water cooled and it had high rotating velocity to minimize fuel pyrolysis

inside the screw. A small N_2 flow (24 L_N/h) was introduced at the start of the screw feeder to prevent any possible reverse flow of volatiles.

The oxygen carrier was decomposed in the fuel reactor, evolving gaseous oxygen into the surroundings. The oxygen burnt the volatiles and char proceeding from fuel pyrolysis in the fuel reactor. Reduced oxygen carrier particles overflowed into the air reactor through a U-shaped fluidized bed loop seal (2 in Fig.2) with a 30 mm inner diameter. A N_2 flow of 60 L_N/h was introduced into the loop seal. Preliminary experiments were carried out to observe the distribution of gas fed into the loop seal. In the experimental conditions used in this work, the gas in the loop-seal was distributed approximately with 50% in each reactor (air and fuel reactor).

The oxidation of the carrier took place in the air reactor (3 in Fig.2), which was a bubbling fluidized bed with an 80 mm inner diameter and 100 mm bed height, followed by a riser (4 in Fig.2) with a 30 mm inner diameter. The air flow was 1740 L_N/h (u_g = 0.40 m/s). In addition, a secondary air flow (240 L_N/h) was introduced at the top of the bubbling bed to assist particle entrainment through a riser. N_2 and unreacted O_2 left the air reactor passing through a high-efficiency cyclone (5 in Fig.2) and a filter before reaching the stack. The oxidized solid particles recovered by the cyclone were sent to a solids reservoir (7 in Fig.2), with the oxygen carrier prepared to start a new cycle. The regenerated oxygen carrier particles returned to the fuel reactor by gravity from the solids reservoir through a solids valve (8 in Fig.2) that controlled the flow rates of solids entering the fuel reactor. A diverting solids valve (6 in Fig.2) located below the cyclone allowed the measurement of the solids flow rates to be taken at any time. Therefore, this design enabled us to control and measure the solids circulation flow rate between both reactors. The ash particles from char combustion were not recovered by the cyclone and were collected in a filter downstream. Thus, ash particles were not accumulated in the

system. Finally, it should be pointed out that leakage of gas between the two reactors was prevented by the presence of the U-shaped loop seal (2 in Fig.2) and the solids reservoir (7 in Fig.2). Thus, the presence of oxygen in the fuel reactor was solely the result of oxygen released by reaction (1 in Fig.2).

The total oxygen carrier inventory in the system was around 2.3 kg, with about 0.7-0.8 kg of this found in the fuel reactor. The amount of solids in the fuel reactor was calculated from pressure drop measurements in the reactor for each test.

CO_2, CO, H_2, CH_4, and O_2 were continuously analysed at the outlet stream from the fuel reactor, whereas CO_2, CO and O_2 were analysed from the flue gases of the air reactor. Non-dispersive infrared (NDIR) analysers (Maihak S710/UNOR) were used for CO, CO_2 and CH_4 concentration determination; a paramagnetic analyser (Maihak S710/OXOR-P) was used to determine O_2 concentration; and a thermal conductivity detector (Maihak S710/THERMOR) was used for H_2 concentration determination. The amount of tar present in the fuel reactor product gas was determined following the tar protocol [31]. Higher C_2, C_3 and C_4 hydrocarbons were analysed off-line by a gas chromatograph (HP5890 Series II).

Because of heat losses, the system was not auto-thermal, and was heated by means of various independent ovens to achieve independent temperature control of the air reactor, fuel reactor and freeboard above the bed in the fuel reactor. During operation, temperatures in the bed and freeboard of the fuel reactor, air reactor bed and riser were monitored, in addition to the pressure drops in important locations of the system, such as the fuel reactor bed, the air reactor bed and the loop seal. The temperature in the fuel reactor was varied from 860 to 935ºC, whereas the freeboard temperature was 900ºC. The temperature in the air reactor was kept at 900ºC.

The solids circulation rate was maintained at a mean value of 4.1 kg/h, while the biomass feeding rate was 0.22 kg/h, corresponding to a power of 1.2 kW. The oxygen carrier to fuel ratio, ϕ, was around 1.2. The oxygen carrier to fuel ratio was defined as the ratio of the oxygen transported by the oxygen carrier to the oxygen demanded by biomass for complete combustion. A value of ϕ = 1 corresponded to the stoichiometric flow of CuO needed to fully convert the fuel to CO_2 and H_2O, with CuO being reduced to Cu_2O. Thus, ϕ was calculated with the following equation:

$$\phi = \frac{R_{OC}\dot{m}_{OC}}{\Omega_{SF}\dot{m}_{SF}} \tag{5}$$

where $\dot{m}_{OC}$ is the solids circulation flow rate in the completely oxidized state and $\dot{m}_{SF}$ is the mass-based flow of the solid fuel fed into the reactor. Ω_{SF} is the stoichiometric kg of oxygen to convert 1 kg of biomass to CO_2 and H_2O. This value was calculated from the proximate and ultimate analysis of biomass, see Table 2, by using the following equation:

$$\Omega_{SF} = \left(\frac{f_C}{M_C} + 0.25\frac{f_H}{M_H} - \frac{f_O}{M_{O_2}} \right) \cdot M_{O_2} \tag{6}$$

where f_i is the mass fraction of the element *i* in biomass.

Air flow into the air reactor was maintained constant for all tests and always exceeded the stoichiometric oxygen demanded by the fuel. The air excess ratio, λ, is defined in equation (7), and the values for the experimental work were always above 1.

$$\lambda = \frac{\text{Oxygen flow}}{\text{Oxygen demanded}} = \frac{0.21F_{air}M_{O_2}}{\Omega_{SF}\dot{m}_{SF}} \tag{7}$$

2.5. Data evaluation

To analyse the reliability of the results, a mass balance to oxygen and carbon was carried out using the measurements of the gas stream coming from the air and fuel

reactors in the continuous CLOU unit. The product gas flow in dry basis in the fuel reactor, F_{outFR}, was calculated as:

$$F_{\mathrm{outFR}} = \frac{F_{\mathrm{inFR}}}{1-(y_{\mathrm{CO_2,outFR}} + y_{\mathrm{CO,outFR}} + y_{\mathrm{H_2,outFR}} + y_{\mathrm{CH_4,outFR}} + y_{\mathrm{O_2,outFR}})} \tag{8}$$

where F_{inFR} is the inlet flow to the fuel reactor, i.e. the sum of N_2 for fluidizing, N_2 from loop seal and N_2 from the screw-feeder, and $y_{i,outFR}$ the i gas concentration exiting from the fuel reactor on a dry basis.

The outlet gas flow from air reactor, F_{outAR}, was calculated by means of the introduced N_2.

$$F_{\mathrm{outAR}} = \frac{F_{\mathrm{N_2,inAR}}}{1-\left(y_{\mathrm{O_2,outAR}} + y_{\mathrm{CO_2,outAR}}\right)} \tag{9}$$

Thus, the exiting flows of O_2 and CO_2 from the air and fuel reactors could be calculated easily using the actual concentration of each gas i:

$$F_{\mathrm{i,out}} = y_{\mathrm{i,out}} F_{\mathrm{out}} \tag{10}$$

Note that nitrogen was used as the fluidizing agent in the fuel reactor during experimental work; thus CO_2 was produced only by the fuel combustion.

With the gas flows, a mass balance to carbon and oxygen can be performed as:

$$\frac{f_{\mathrm{C}}}{M_C}\dot{m}_{\mathrm{SF}} = (F_{\mathrm{CO_2,outFR}} + F_{\mathrm{CO,outFR}} + F_{\mathrm{CH_4,outFR}}) + F_{\mathrm{CO_2,outAR}} + F_{C,elut} \tag{11}$$

$$M_{\mathrm{O_2}}\left(F_{\mathrm{CO_2,outFR}} + F_{\mathrm{O_2,outFR}} + 0.5F_{\mathrm{CO,outFR}} + 0.5F_{\mathrm{H_2O,outFR}}\right)_{\mathrm{outFR}} - \left(\frac{f_{\mathrm{H_2O}}}{M_{\mathrm{H_2O}}} + \frac{f_{\mathrm{O}}}{M_{\mathrm{O}}}\right)\dot{m}_{\mathrm{SF}} = \\ = M_{\mathrm{O_2}}\left[F_{\mathrm{O_2,inAR}} - \left(F_{\mathrm{O_2,outAR}} + F_{\mathrm{CO_2,outAR}}\right)\right] \tag{12}$$

where $F_{C,elut}$ is the flow of carbon elutriated from the fuel reactor as unburnt char.

Water concentration was not measured. However, in order to take into account the oxygen exiting with H_2O resulting from the oxidation of hydrogen in the fuel, it was assumed that water came both from the humidity and hydrogen content in fuel:

$$F_{\mathrm{H_2O,outFR}} = \left(0.5\frac{f_H}{M_{\mathrm{H}}} + \frac{f_{\mathrm{H_2O}}}{M_{\mathrm{H_2O}}} \right) \dot{m}_{\mathrm{SF}} - F_{H_2,outFR} \tag{13}$$

The evaluation of the CLOU performance with solid fuels was carried out by studying the effect of the operational variables on CO_2 capture efficiency, char conversion and combustion efficiency in the fuel reactor.

CO_2 capture efficiency, η_{CC}, is defined as the fraction of carbon present in the fuel at the outlet of fuel reactor. This is the real CO_2 captured in the CLOU system, as the remaining carbon exits as CO_2 together with nitrogen at the air reactor outlet:

$$\eta_{CC} = 1 - \frac{F_{\mathrm{CO_2,outAR}}}{\frac{f_C}{M_C}\cdot\dot{m}_{SF}} \tag{14}$$

CO_2 capture efficiency depends on the conversion of char in the fuel reactor, X_{char}. Its value is calculated by considering that the carbon in gases from the fuel reactor comes from the carbon in volatiles and carbon in converted char. Thus, the carbon from reacting char was the inlet carbon minus the flow of carbon in volatiles, $F_{\mathrm{C,vol}}$, and in elutriated char particles, $F_{C,elut}$:

$$X_{\mathrm{char}} = \frac{F_{\mathrm{CO_2,outFR}} + F_{\mathrm{CO,outFR}} + F_{\mathrm{CH_4,outFR}} - F_{\mathrm{C,vol}}}{F_{\mathrm{CO_2,outFR}} + F_{\mathrm{CO,outFR}} + F_{\mathrm{CH_4,outFR}} + F_{\mathrm{CO_2,outAR}} - F_{\mathrm{C,vol}}} \tag{15}$$

The molar flow of carbon contained in the volatile matter was calculated as:

$$F_{\mathrm{C,vol}} = \frac{\left(f_{\mathrm{C}} - f_{C,fix} \right)\dot{m}_{\mathrm{SF}}}{M_{\mathrm{C}}} \tag{16}$$

where $f_{\mathrm{C,fix}}$ is the fixed carbon given by fuel analysis, see Table 2. Eq. (16), assuming that the volatiles evolving in the fuel reactor are the same as those in the proximate analysis measurement.

The conversion of char in the fuel reactor was related to the temperature and the mean residence time of solids in the fuel reactor, τ_{FR}, calculated by the following equation:

$$\tau_{FR} = \frac{m_{s,FR}}{\dot{m}_{OC}} \quad (17)$$

where $m_{s,FR}$ is the mass of solids in the fuel reactor and $\dot{m}_{OC}$ the solids circulation rate between the air and fuel reactors.

The fractional conversion rate of the char, ($-r_C$), can be calculated from the values of the char conversion in the fuel reactor and the mean residence time of char particles in this reactor, τ_{char}. The fractional conversion rate of char was calculated as follows:

$$(-r_c) = \frac{X_{char}}{\tau_{char}} \quad (18)$$

τ_{char} is related to the mean residence time of solids in the fuel reactor with the following equation:

$$\tau_{char} = \tau_{FR} \cdot (1 - X_{char}) \quad (19)$$

Finally, combustion efficiency in the fuel reactor, $\eta_{comb,FR}$, evaluates the degree of combustion with respect to the fraction of fuel converted in the fuel reactor. The combustion efficiency in the fuel reactor was calculated through the quotient between the oxygen required to fully burn unconverted gases (CH_4, CO and H_2) and the oxygen demanded for complete combustion of the biomass converted in the fuel reactor. Therefore, the combustion efficiency in the fuel reactor was calculated as:

$$\eta_{comb,FR} = 1 - \frac{4F_{CH_4,outFR} + F_{CO,outFR} + F_{H_2,outFR}}{2\Omega_{SF}\dot{m}_{SF} - 2F_{CO_2,outAR} - 2F_{C,elut}} \quad (20)$$

3. Results

3.1. Biomass combustion

To investigate the combustion of biomass by a CLOU system, different tests were carried out under continuous operation in the ICB-CSIC-s1 experimental rig. Cu60MgAl material was used as the oxygen carrier. The effect of the fuel reactor temperature on the combustion efficiency and CO_2 capture efficiency was investigated. Thus, the fuel reactor temperature was varied from 860ºC to 935ºC. A total of 10 h of operation were carried out without agglomeration of the oxygen carrier.

The composition of the exit gases from the fuel and air reactors was determined for every experimental condition. As an example, Fig. 3 shows the concentration of gases (dry basis) measured as a function of the operating time. Several temperatures in the fuel reactor were tested, and each was maintained at steady state for at least 120 min.

When temperature was varied, a transition period appeared and stable combustion was reached usually in less than 10 min. The steady state was reached when the oxygen transferred from the oxygen carrier to the fuel was equal to the oxygen transferred from the air to the oxygen carrier. At steady state, the gas outlet concentration and temperature were maintained uniform throughout the entire combustion time. The mass balances for carbon and oxygen, see Eqs. (11) and (12), were found to be accurate, closing at 95%. Thus, the loss of carbon by elutriation of char particles from the fuel reactor or carbon not recovered by cyclone was negligible with regard to the carbon balance in the system.

For the test carried out at the lower fuel reactor temperature, 860ºC, there was a high concentration of CO in the fuel reactor outlet gas stream, and the oxygen concentration was near 0. The only unburnt gaseous product was CO; neither CH_4 nor

H_2 were found at the fuel reactor outlet. These results agreed with those found by Adánez et al. [32] during fluidized bed biomass combustion. They reported CO being the main volatile product during pine wood devolatilization. Moreover, CO was an intermediate product during volatile combustion, with a lower combustion rate than CH_4 and H_2. All these reasons would justify that the main unburnt product was CO at the lowest temperature in the CLOU experiments.

Besides the large production of volatiles, significant amount of tar compounds can be generated during biomass processing. In order to study the fate of the tar compounds generated during biomass CLOU combustion in the CLC unit, samples were taken at different temperatures according to the tar protocol. Tar compounds were only measured at 860ºC, at a concentration of 0.31 g/Nm^3 (dry basis). The composition of these tars were mainly naphthalene (61.7 wt.%), phenantrene (13.1 wt.%), acenaphthylene (12.5 wt.%) indene (7.2 wt.%) and stryrene (5.5 wt.%). The amount of tar detected in this work during biomass CLOU combustion was four times lower than that found by Mendiara et al. [29] in *i*G-CLC combustion using the same biomass and similar operating temperature (880ºC). Moreover, the tar composition was different, as it was mainly composed of naphthalene in the biomass *i*G-CLC process [29]. The tar content in the fuel reactor exhaust gas may have implications for the further steps of compression, transport and storage, since operational problems may be anticipated if the tar concentration is high. Tar condenses easily, and this property is known to cause fouling in pipes, filter elements and heat exchangers. To prevent these problems, Reed et al. [33] gave an interval of tar concentration between 0.05 to 0.5 g/Nm^3, for compressing and piping biomass processed gas. According to those limits, the tar content of the FR gas exhaust measured in this work at all temperatures were below those limit values, and thus no additional gas conditioning step should be required.

As was expected given the thermodynamics, the oxygen uncoupling effect at this temperature was low. At the same time, the unburnt char was transferred to the air reactor together with the oxygen carrier particles. There, the char was burnt and the oxygen carrier was regenerated. So, CO_2 appeared as a combustion product from the air reactor.

When the fuel reactor temperature was higher than 900ºC, there was significant O_2 release due to the CLOU effect and no CH_4, CO or H_2 were detected in the gases exiting from the fuel reactor. The possible presence of tars or light hydrocarbons was also analysed. The results showed that there were no tars in the fuel reactor outlet flow, i.e. no hydrocarbons heavier than C_5 at temperatures higher than 900 ºC. Furthermore, in these experiments, gas from the outlet stream of fuel reactor was collected in bags and analysed with a gas chromatograph. The analysis showed that there were no C_2-C_4 hydrocarbons in the gases. Thus, CO_2, H_2O and O_2 were the only gases, together with N_2 introduced as the fluidizing gas at high temperature. Moreover, very low fractions of NO were present in the gases coming from nitrogen present in the biomass. However, nitrogen components were not evaluated in this work. Special experiments should be performed to eliminate any N_2 flow into the fuel reactor to estimate NO_x formation in a CLC system [34].

Fig. 4(a) shows the combustion and CO_2 capture efficiencies obtained in the plant as a function of the fuel reactor temperature. Complete combustion of biomass to CO_2 and H_2O was found in the fuel reactor for the experiments at temperatures higher than 900ºC. The solids inventory in the fuel reactor was 565 kg/MW_{th} in all tests. Nevertheless, complete combustion can be expected with a lower solids inventory. At temperatures lower than 900ºC, 82% of combustion efficiency was obtained, and there were CO and tars presents at the outlet of fuel reactor. Unburnt compounds come

mainly from volatile matter, as was shown in previous work in this CLC unit [35]. Biomass contains 81% volatile matter, therefore, the high volatile matter content of the biomass is responsible for the low combustion efficiency showed at the lowest temperature. Note that unburnt compounds are always present at the outlet of the fuel reactor for materials without oxygen uncoupling properties, even if highly reactive materials or a high solids inventory were used [12, 20]. Similar combustion behaviour was obtained in *i*G-CLC made with biomass using an iron based oxygen carrier, i.e. $\eta_{comb,FR}$ = 80% at 880ºC with 1550 kg/MW_{th}. With the Cu-based material used in this work, $\eta_{comb,FR}$ = 82% but with much lower amount of solids (565 kg/MW_{th}), highlighting the high reactivity of the Cu-based material.

To understand the differences on performance at temperatures lower or higher than 900ºC, it is necessary to take into account that O_2 generated from CuO increases with temperature. This fact is related to the increase in both reaction rate and equilibrium O_2 concentration. At temperatures ≥ 900ºC, O_2 released from the oxygen carrier should be of great relevance for the conversion of gaseous compounds proceeding from coal devolatilization. Thus, volatile matter reacts with gaseous O_2 from the oxygen uncoupling mechanism in a homogeneous reaction. On contrary, at 860ºC, the O_2 generated is extremely low (equilibrium O_2 concentration is 0.5 vol.%). Thus, the gas conversion by a direct gas-solid reaction with the oxygen carrier could be the more relevant mechanism at the lower temperature. At this temperature, oxygen carrier reduction to generate gaseous O_2 is extremely slow [36]. The lack of the oxygen uncoupling is responsible for the relatively low combustion efficiency present in the fuel reactor under these conditions. Nevertheless, it should be noted that the contact between volatile matter and oxygen carrier particles can be poor because they are likely to be generated in a plume. Consequently, gas-solid contact must be seen as a limiting

step during combustion of volatile matter instead of the low reactivity of gases with the oxygen carrier material. The presence of a volatile plume and low amounts of solids in the freeboard of this CLC unit [35] is believed to be critical for the low gas conversion at low temperature. Note that when the gas-solid contact is improved, e.g. during combustion of gaseous fuels in previous works [37, 38], complete combustion can be achieved at conditions where oxygen uncoupling is not relevant.

In order to obtain complete combustion, an oxygen uncoupling effect is needed. Thus, it was found that volatiles were fully converted into CO_2 and H_2O in the fuel reactor at temperatures higher than 900ºC by reaction with the oxygen released from CuO decomposition. In addition, the oxygen release rate was high enough to supply an excess of gaseous oxygen (O_2), which exited together with the combustion gases. The oxygen concentration was at equilibrium conditions for each reactor temperature. At the same time, the O_2 concentration at the air reactor outlet decreased slightly with temperature owing to the oxygen carrier becoming more reduced from the fuel reactor because more oxygen was released there.

CO_2 capture efficiencies are dependent on the carbon transferred in char particles from the fuel to the air reactor. CO_2 capture efficiency increases with the fuel reactor temperature. Thus, high carbon capture efficiencies were found at fuel reactor temperatures higher than 900ºC, reaching 100% efficiency at 935ºC. As all the carbon in the volatiles was burnt in the fuel reactor, the carbon capture depended only on the unconverted char in the fuel reactor, i.e. on the char conversion, which in a CLOU or a CLC system is dependent on the fuel reactor temperature and the solids circulation flow rate [39]. Nevertheless, the solids flow rate was maintained constant for all the tests. Fig 4(b) shows the char conversion in the fuel reactor as a function of the fuel reactor temperature. The char conversion increased with the fuel reactor temperature because of

the higher char combustion rates. However, low char conversion can be seen at the lowest temperature when only 15% of char conversion is reached in the fuel reactor and there is no gaseous O_2 in the fuel reactor exiting flow. However, the 80% of CO_2 capture efficiency obtained was due to the high amount of volatiles in the biomass composition. This important decrease in the char conversion can be attributed to a change in the mechanism for the combustion of char. At the lower temperature, 860ºC, the oxygen uncoupling effect is low because the O_2 equilibrium concentration is low and the oxygen generation rate by the oxygen carrier particles is low. So the conversion rate of char by combustion reaction should be low. Char conversion is mainly driven at this temperature by the slow gasification reaction with the low H_2O or CO_2 concentration inside the fuel reactor.

As the temperature increases, the oxygen uncoupling effect increases. Thus, the O_2 equilibrium at 900ºC is 1.5 vol.%. But what is more relevant is the high oxygen generation rate that the oxygen carrier shows at temperatures higher than 900ºC [16]. As a consequence, the rate of char combustion is directly increased.

This work presents the first experimental hours of burning biomass by means of a CLOU process in a continuous unit. Although the total operation time carried out (10 h) was not long enough for application on an industrial scale, it was sufficiently relevant from the research point of view, since no important drawbacks were found for the process. A future experimental campaign involving the burning of different types of biomass, such as almonds shells, olive stones and corn stover, is planned in order to extend the evaluation of the CLOU process with other biomasses.

3.2 Characterization of used Cu60MgAl oxygen carrier particles

Samples of solids extracted from the fuel and air reactors after 10 h of continuous operation in the CLOU unit were characterized by different techniques. Table 1 shows relevant properties for used particles compared to the fresh ones.

The XRD analysis of used particles revealed the presence of CuO and $MgAl_2O_4$ as major components. Thus, no changes were observed in the chemical structure of the material. In addition, XRD results of some reduced samples taken from the fuel reactor of the CLOU unit at different times showed only Cu_2O and $MgAl_2O_4$ as the main components. In other words, metallic Cu was never detected in the samples, even in those tests where the variation of the solids conversion was close to unity.

The used particles had a stable CuO content of 60 wt.%, similar to the fresh ones. In addition, reactivity data were obtained in TGA tests from the mass variations during the reduction and oxidation cycles as a function of time. The oxygen carrier reduction conversion was calculated as $X_{red} = (m_{ox}–m)/(m_{ox}–m_{red})$ and $X_{ox} = 1–X_{red}$ where m is the mass of sample at each time, m_{ox} is the mass of the fully oxidized sample, and m_{red} is the mass of the sample in the reduced form. Fig. 5 shows the conversion vs. time curves obtained for the decomposition and oxidation reactions for the used samples, as well as for fresh oxygen carrier. The maintenance of the initial reactivity can be clearly seen for used particles both in decomposition and oxidation reactions. This fact justifies their unchanged ability to release oxygen at equilibrium conditions and to be re-oxidized by air observed in the CLOU unit after the large number of reduction-oxidation cycles the oxygen carrier particles underwent.

SEM images of fresh and used particles after 10 h of operation in the CLOU unit are shown in Figure 6. No significant changes were observed in the particles after operation with biomass. EDX analysis showed that internal CuO distribution inside the

particles was uniform and was unchanged. Moreover, the rich alkalimetal composition of the biomass ashes (see Table 2) had the potential to produce agglomeration problems in the fuel reactor, owing to bed sintering that can block solids circulation between reactors. Fig 6(c) of the used oxygen carrier particles shows that no agglomerate resulted from the interaction between the ash compounds and the oxygen carrier, which was in line with the avoidance of tendency towards agglomeration during all the operating time. It must be pointed out that the oxygen carrier particles never showed agglomeration problems, even when the oxygen carrier was highly reduced. EDX analysis of the used particles, Fig 6(d), was conducted on the surface of the particles in order to test for the presence of alkali metals from biomass ashes (Ca, K, P, Na). No evidence was found of ash deposition on the oxygen carrier particles, being the EDX profile similar to that obtained for fresh particles; see Fig 6(b). However, it is necessary to highlight that the combination of a short operating time (10 h) and the elutriation of the ash particles would result in a low contacting time between ash and oxygen carrier particles, which could be not representative of the behaviour in an industrial CLOU unit. Specific test would be requested to assess the interaction of ash component with oxygen carrier particles.

In addition, a reduction was found in the crushing strength of the particles as operation time increased, which agreed with previous results found with this material [25]. The reduction in the crushing strength of the particles was associated with an increase in porosity as the operation time in the CLOU unit increased, see Table 1. The durability of this material was in line with results shown in a previous work [25], where the crushing strength decreased to 1.5 N after 18 h of operation. However, fines particles (<40 μm) were not found neither in the fuel reactor nor in the air reactor. No

differences on the evolution of these properties were observed whatever coal or biomass was used as fuel.

4. Discussion

From results presented in this work, char conversion in the fuel reactor is a relevant issue affecting CO_2 capture efficiency in the CLOU process, even where a fuel with a high volatile content is used, as it is the case of biomass. In order to analyse the conversion degree of biomass char in the CLC technology, a deep study was carried out that included char conversion rates obtained in the CLOU process when different fuels were used. Thus, carbon capture efficiency was analysed by means of the fractional conversion rate of char of different solid fuels, including data from Adánez-Rubio et al. [26] for coals ranging from anthracite to lignite. Also the biomass char conversion rate obtained from the *i*G-CLC process by Mendiara et al [29] was considered for comparison purposes.

The fractional conversion rate of char per unit of carbon mass in char can be used to carry out a comparison between the different fuels, because char conversion in the fuel reactor, and hence carbon capture, depends directly on this rate. Fig. 7 shows the fractional conversion rate of char as a function of temperature calculated using Eq. (18) for the biomass and coal fuels used in the CLOU unit [26]. As expected, the fractional conversion rate of char increased with temperature. It can be observed that the conversion rate for biomass char in the CLOU process was very similar to that obtained for lignite, the most reactive coal tested in the CLOU unit. This high conversion rate for biomass char, together with the large amount of volatile matter content in biomass, allows very high carbon capture efficiencies to be achieved, even higher than those obtained for lignite under the same conditions. In addition, the biomass char conversion

rate in CLOU was higher than that obtained in *i*G-CLC. The char conversion rate for biomass in the CLOU process was 3 to 4 times higher than that obtained in the *i*G-CLC process at temperatures equal to or higher than 900ºC. This was due to the different char conversion mechanisms. In CLOU, char was converted by combustion with gaseous oxygen, while *i*G-CLC involved a slow char gasification process with steam or CO_2. This higher char conversion rate in the CLOU process explained the lower oxygen carrier inventories needed in CLOU (565 kg/MW_{th}) compared to those required by *i*G-CLC (1550 kg/MW_{th}) [29] to obtain similar carbon capture efficiencies (97.5/99%). However, at the lowest temperature for CLOU process (860ºC) the char conversion rate was lower than the rate for *i*G-CLC. This may be due to: (a) no gasification agent (steam or CO_2) is fed into the CLOU fuel reactor, and (b) there was no gaseous oxygen at this temperature to burn the char.

Char conversion in the fuel reactor can be calculated as a function of the solid inventory, solids circulation rate and char conversion rate as follows [26]:

$$X_{char} = 1 - \frac{\dot{m}_{OC}(1-\eta_{CSS})}{(-r_C)\cdot m_{s,FR} + \dot{m}_{OC}(1-\eta_{CSS})} \quad (21)$$

In Eq. (21) the incorporation of a carbon separation system, similar to the iG-CLC process, was considered by using the parameter η_{CCS} , i.e. carbon separation system efficiency. Carbon capture efficiency is related to the char conversion through the following equation:

$$\eta_{CC} = \frac{f_{C,vol}}{f_C} + \frac{f_{C,char}}{f_C}\cdot X_{char} = \frac{f_C - f_{C,fix}}{f_C} + \frac{f_{C,fix}}{f_C} X_{char} \quad (22)$$

Using Eqs. (21) and (22), it was possible to analyse the effect of the oxygen carrier inventory on char conversion and carbon capture efficiency in the system, once the value of $(-r_C)$ was known. In this analysis, the residence time of solids was maximized by operating at a value of the oxygen carrier to fuel ratio, ϕ = 1.1, thus

maximizing the CO_2 capture rate in a CLC unit [18, 39]. Therefore, the solid circulation flow rate per MW_{th} of fuel was fixed. With regard to the CLOU process with biomass, Fig. 8 shows carbon capture efficiency as a function of the oxygen carrier inventory in the fuel reactor for two different fuel reactor temperatures without implementing a carbon separation system ($\eta_{CSS} = 0$). Carbon capture efficiency increased with the fuel reactor solids inventory due to the increase in char conversion. An increase in the fuel reactor temperature also increased the char conversion rate. It is evident that a carbon capture efficiency higher than 95% can be achieved with a very low amount of oxygen carrier inventories (230 and 110 kg/MW_{th} for 900 and 920ºC, respectively). Therefore, the use of a carbon separation system is not necessary for the CLOU process when biomass is used as fuel.

5. Conclusions

The performance of CLOU burning a biomass fuel with a Cu-based oxygen carrier was analysed in a continuous unit. A fuel reactor temperature higher than 900ºC was required to exploit the oxygen uncoupling benefits and resulting in no unburnt compounds at the fuel reactor outlet. Complete combustion and 100% CO_2 capture efficiency were achieved at a fuel reactor temperature of 935ºC using a low solids fuel reactor inventory. The conversion rate of biomass char was analysed, and for the CLOU process it was found to be very similar to that obtained with lignite. Moreover, the char conversion rate of biomass in the CLOU process is between 3 and 4 times higher than that corresponding to the *i*G-CLC process at temperatures above 900ºC.

With the results obtained in the continuous CLOU unit, an optimization of the CLOU process was carried out to maximize CO_2 capture efficiency with a minimum solid inventory. A carbon capture efficiency higher than 95% can be achieved with a

very low amount of oxygen carrier inventories (230 and 110 kg/MW_{th} for 900 and 920ºC respectively) and without the need for a carbon separation system. These encouraging results, first obtained with pine wood biomass in the CLOU process, indicate that studied should be carried out on the use of other types of biomass fuels with CLC technology.

ACKNOWLEDGEMENTS

This work was partially supported by the European Commission, under the RFCS program (ACCLAIM Project, Contract RFCP-CT-2012-00006), and by the Spanish MICINN (ENE2011-26354). I. Adánez-Rubio thanks CSIC for the JAE fellowship co-financed by the European Social Fund.

NOTATION

Symbols

F_i	Molar flow of compound i (mol/s)
f_C	Mass fraction of carbon in coal (-)
$f_{C,fix}$	Mass fraction of fixed carbon in biomass (-)
$f_{C,vol}$	Mass fraction of carbon in volatiles (-)
f_i	Mass fraction in fuel of element or compound i (-)
M_i	Atomic or molecular weight of i elements or compounds (kg/mol)
$\dot{m}_{SF}$	Mass-based flow of solid fuel fed into the fuel reactor (kg/s)
$\dot{m}_{OC}$	Solids circulation rate (kg/s)
m_{ox}	Mass of the fully oxidized oxygen carrier sample (kg)
m_{red}	Mass of the fully reduced oxygen carrier sample (kg)
$m_{s,FR}$	Mass of solids in the fuel reactor (kg)
$(-r_C)$	Fractional conversion rate of the char (s^{-1})
τ_{char}	Mean residence time of char particles in the fuel reactor (s)
τ_{FR}	Mean residence time of solids in the fuel reactor (s)
R_{OC}	Oxygen transport capacity (-)
X_{char}	Carbon Conversion in char particles (-)
y_i	Molar fraction of the gas i (-)

Greek letters

η_{CC}	CO_2 capture efficiency (-)
$\eta_{comb,FR}$	Combustion efficiency in the fuel reactor (-)

η_{CSS}	Efficiency of the carbon separation system (-)
λ	Air excess ratio (-)
ϕ	Oxygen carrier to fuel ratio (-)
Ω_{SF}	Stoichiometric mass of O_2 to convert 1 kg of solid fuel (kg/kg)

Subscripts

AR	Air reactor
char	Carbon in char particles
elut	Elutriated particles from fuel reactor
FR	Fuel reactor
inAR	Inlet stream to air reactor
inFR	Inlet stream to fuel reactor
outAR	Outlet stream from air reactor
outFR	Outlet stream from fuel reactor
OC	Oxygen carrier
SF	Solid fuel
vol	Volatile matter

Acronyms

BET	Brunauer-Emmett-Teller
CCS	CO_2 Capture and Storage
CLC	Chemical Looping Combustion
CLOU	Chemical Looping with Oxygen Uncoupling
IPCC	Intergovernmental Panel on Climate Change
LHV	Low Heating Value (kJ/kg)

TGA	Thermogravimetric analyser
XRD	X-ray diffractometer

REFERENCES

[1] IPCC, IPCC special report on carbon dioxide capture and storage, in: B. Metz, O. Davidson, H.C. de Coninck, M. Loos and L.A. Meyer, (Eds), Working group III of the intergovernmental panel on climate change, Cambridge University, 2005.

[2] H.R. Kerr, Carbon Dioxide Capture for Storage in Deep Geologic Formations, In: Thomas DC, Benson SM (Eds.), Capture and Separation Technology Gaps and Priority Research Needs, Elsevier Science, Amsterdam, 2005, pp. 655-660.

[3] H.M. Kvamsdal, K. Jordal, O.Bolland, A quantitative comparison of gas turbine cycles with CO_2 capture, Energy 32(1) (2007) 10-24.

[4] J. Adánez, A. Abad, F. Garcia-Labiano, P. Gayán, L.F. de Diego, Progress in Chemical-Looping Combustion and Reforming Technologies, Prog. Energy Comb. Sci. 38 (2012) 215-282.

[5] A. Lyngfelt, Oxygen carriers for chemical looping combustion -4000 h of operational experience, Oil & Gas Sci Tech 66 (2011) 161-172.

[6] Y. Cao and W.P. Pan, Investigation of chemical looping combustion by solid fuels. 1. Process analysis, Energy Fuels 20 (2006) 57-68.

[7] S.A Scott, J.S Dennis, A.N Hayhurst, T. Brown, In Situ Gasification of a Solid Fuel and CO_2 Separation using Chemical Looping, AIChE J. 52 (2006) 3325-3328.

[8] N. Berguerand, A. Lyngfelt, Design and operation of a 10 kW_{th} chemical-looping combustor for solid fuels - Testing with South African coal, Fuel 87 (2008) 2713-2726.

[9] L. Shen, J. Wu, J. Xiao, Experiments on chemical looping combustion of coal with a NiO based oxygen Carrier, Combustion and Flame 156 (2009) 721-728.

[10] P. Markström, C. Linderholm, A. Lyngfelt, Chemical-looping combustion of solid fuels-Design and operation of a 100 kWth unit with bituminous coal, Int. J. Greenhouse Gas Control 15 (2013) 150-162.

[11] A. Cuadrat, A. Abad, F. García-Labiano, P. Gayán, L.F. de Diego, J. Adánez, Relevance of the coal rank on the performance of the in-situ Gasification Chemical-Looping Combustion, Chem. Eng. J. 195-196 (2012) 91-102.

[12] P. Gayán, A. Abad, L.F. de Diego, F., García-Labiano, J. Adánez, Assessment of technological Solutions for improving Chemicals Looping Combustion of solid fuel with CO_2 capture, Chem. Eng. J. 233 (2013) 56-69.

[13] T. Mattisson, A. Lyngfelt, H. Leion, Chemical-looping oxygen uncoupling for combustion of solid fuels, Int J Greenhouse Gas Control 3 (2009) 11-19.

[14] W.K. Lewis, E.R., Gilliland, Production of pure carbon dioxide. Patent 2665972, (1954).

[15] A. Abad, I. Adánez-Rubio, P. Gayán, F. García-Labiano, L.F. de Diego, J. Adánez, Demonstration of chemical-looping with oxygen uncoupling (CLOU) process in a 1.5 kW_{th} continuously operating unit using a Cu-based oxygen-carrier, International Journal of Greenhouse Gas Control 6 (2012) 189-200.

[16] I. Adánez-Rubio, P. Gayán, A. Abad, L.F. de Diego, F. García-Labiano, J. Adánez, Identification of Operational Regions in the Chemical-Looping with Oxygen Uncoupling (CLOU) Process with a Cu-based Oxygen-Carrier, Fuel 102 (2012) 634-645.

[17] A. Cuadrat, A. Abad, L.F. de Diego, F., García-Labiano, P., Gayán, J., Adánez, Prompt considerations on the design of Chemical-Looping Combustion of coal from experimental tests, Fuel 97 (2012) 219-232.

[18] A. Cuadrat, A. Abad, P. Gayán, L.F. de Diego, F. García-Labiano, J. Adánez, Theoretical approach on the CLC performance with solid fuels: Optimizing the solids inventory, Fuel 97(2012) 536-551.

[19] A. Abad, P. Gayán, L.F. de Diego, F. García-Labiano, J. Adánez, Fuel reactor modelling in chemical-looping combustion of coal: 1. model formulation, Chem. Eng. Sci. 87 (2013) 277-293.

[20] F. García-Labiano, L.F. de Diego, P., Gayán, A., Abad, J., Adánez, Fuel reactor modelling in chemical-looping combustion of coal: 2. simulation and optimization, Chem. Eng. Sci. 87 (2013.) 173-182.

[21] P. Gayán, I. Adánez-Rubio, A. Abad, L.F. de Diego, F. García-Labiano, J. Adánez, Development of CuO-based oxygen-carrier materials suitable for Chemical-Looping with Oxygen Uncoupling (CLOU) process, Fuel 96, (2012) 226-238.

[22] I. Adánez-Rubio, M. Arjmand, H. Leion, P. Gayán, A. Abad, T. Mattisson, A. Lyngfelt, Investigation of Combined Supports for Cu-based Oxygen Carriers for Chemical-Looping with Oxygen Uncoupling (CLOU), Energy Fuels 27 (2013) 3918-3927.

[23] T. Mattisson, Materials for Chemical-Looping with Oxygen Uncoupling, ISRN Chemical Engineering, (2013) Article ID 526375 (http://dx.doi.org/10.1155/2013/526375).

[24] Q. Imtiaz, D. Hosseini, C.R. Müller, Review of Oxygen Carriers for Chemical Looping with Oxygen Uncoupling (CLOU): Thermodynamics, Material Development, and Synthesis, Energy Technol. 1 (2013) 633-647.

[25] I. Adánez-Rubio, P. Gayán, A. Abad, L.F. de Diego, F. García-Labiano, J. Adánez, Evaluation of a Spray-Dried $CuO/MgAl_2O_4$ Oxygen Carrier for the Chemical Looping with Oxygen Uncoupling Process, Enegy Fuels 26 (2012) 3069-3081.

[26] I. Adánez-Rubio, A. Abad, P. Gayán, L.F. de Diego, F. García-Labiano, J. Adánez, Performance of CLOU process in the combustion of different types of coal with CO_2 capture, Int. J. Greenhouse Gas Control 12 (2013) 430-440.

[27] I. Adánez-Rubio, A. Abad, P. Gayán, F., García-Labiano, L.F. de Diego, J. Adánez, The fate of sulphur in the Cu-based Chemical Looping with Oxygen Uncoupling (CLOU) Process, Applied Energy 113 (2014) 1855-1862.

[28] H. Gu, L. Sheng, J. Xiao, S. Zhang, T. Song, Chemical looping combustion of biomass/coal with natural iron ore as oxygen carrier in a continuous reactor. Energy Fuels 25 (2011) 446-455.

[29] T. Mendiara, A. Abad, L.F. de Diego, F. García-Labiano, P. Gayán, J. Adánez, Biomass combustion in a CLC system using an iron ore as oxygen carrier, Int. J. Greenhouse Gas Control 19 (2013) 322-330.

[30] L. Shen, J. Wu, J. Xiao, Q. Song, R. Xiao, Chemical-Looping Combustion of Biomass in a 10 kW_{th} Reactor with Iron Oxide As an Oxygen Carrier, Energy Fuels 23 (2009) 2498-2505.

[31] P. Simell, P. Stahlberg, E. Kurkela J. Albretch S. Deutch K. Sjostrom, Provisional protocol for the sampling and analysis of tar and particulates in the gas from large-scale biomass gasifiers, Version 1998, Biomass and Bioenergy 18 (2000) 19-38.

[32] J. Adánez, P. Gayán, L.F. de Diego, F. García-Labiano, A. Abad, Combustion of wood chips in a CFBC. Modeling and validation, Ind. Eng. Chem. Res. 42(5) (2003) 987-999.

[33] T.B Reed, B. Levie, M.S. Graboski, Tar conversion, in: Fundamentals, Development and Scaleup of the Air-Oxygen Stratified Downdraft Gasifier, Solar Energy Research Institute, SERI/PR-234-2571, 1987.

[34] T. Mendiara, M.T. Izquierdo, A. Abad, L.F. de Diego, F. García-Labiano, P. Gayán, J. Adánez, Release of pollutant components in CLC of lignite, Int. J. Greenhouse Gas Control 22 (2013) 15-24

[35] A. Cuadrat, A. Abad, F. García-Labiano, P. Gayan, L.F. de Diego, J. Adánez, The use of ilmenite as oxygen-carrier in a 500 W_{th} Chemical-Looping Coal Combustion unit, Int J Greenhouse Gas Control 5 (2011) 1630-1642.

[36] I. Adánez-Rubio, P. Gayán, A. Abad, F. García-Labiano, L.F. de Diego, J. Adánez, Kinetics of a Cu-based Oxygen Carrier for Chemical Looping with Oxygen Uncoupling (CLOU): relevance of temperature and oxygen partial pressure on reduction and oxidation, Submited for publication.

[37] J. Adánez, P. Gayán, J. Celaya, L.F. de Diego, F. García-Labiano, A. Abad, Chemical looping combustion in a 10 kW_{th} prototype using a CuO/Al_2O_3 oxygen carrier: effect of operating conditions on methane combustion, Ind. Eng. Chem. Res. 45(17) (2006) 75-80.

[38] C.R. Forero, P. Gayán, L.F. de Diego, A. Abad, F. García-Labiano, J. Adánez, Syngas combustion in a 500 W_{th} Chemical-Looping Combustion system using an impregnated Cu-based oxygen carrier. Fuel Proc. Tech. 90 (2009) 1471-1479.

[39] A. Cuadrat, A. Abad, F. García-Labiano, P. Gayán, L.F. de Diego, J. Adánez, Effect of operating conditions in Chemical-Looping Combustion of coal in a 500 W_{th} unit. Int. J. Greenhous Gas Control 6 (2012) 153-163.

Caption of Tables

Table 1 Properties of the fresh and used oxygen carrier Cu60MgAl.

Table 2. Properties of biomass used in this work; including ash composition (wt%).

Table 1. Properties of the fresh and used oxygen carrier Cu60MgAl.

	Techniques	Fresh	Used
CuO content (wt.%)	TGA, CI Electronics	60	60
Oxygen transport capacity, R_{OC} (wt.%)	TGA, CI Electronics	6	6
Crushing strength (N)	Dynamometer, Shimpo FGN-5X	2.4	1.9
Skeletal density (kg/m^3)	He picnometry, Micromeritics AccuPyc II 1340	4600	4651
Porosity (%)	Hg intrusion, Quantachrome PoreMaster 33	16.1	22.8
Specific surface area, BET (m^2/g)	BET method, Micromeritics ASAP-2020	< 0.5	0.5
XRD main phases	Diffractometer , Bruker AXS	CuO, $MgAl_2O_4$	CuO, $MgAl_2O_4$

Table 2. Properties of biomass used in this work; including ash composition (wt%).

Proximate Analysis (wt.%)		**Ultimate Analysis (wt.%)**	
Moisture	4.2	C	51.4
Volatile matter	81.0	H	6.5
Fixed carbon	14.4	N	0.3
Ash	0.4	S	0.0
		O[(1)]	37.2
Ash composition			
Al_2O_3	2.4	Na_2O	0.2
CaO	40.7	SiO_2	6.6
Fe_2O3	1.3	TiO_2	0.1
K_2O	8.9	MnO_2	0.8
MgO	6.6	P_2O_5	1.6
LHV (kJ/kg)	19186		
Ω_{SF} (kg O_2/kg solid fuel)	1.4		

[(1)]Oxygen to balance

Caption of figures:

Fig. 1. Schematic layout of the CLOU system.

Fig. 2. Schematic view of the ICB-CSIC-s1 unit for the CLOU process (1.5 kW_{th}).

Fig. 3. Evolution of the gas composition in the air and fuel reactor as temperature in the fuel reactor was varied. $\dot{m}_{SF} = 0.24\ kg/h$.

Fig. 4. (a) Combustion efficiency in the fuel reactor and CO_2 capture efficiency and (b) char conversion, as a function of the fuel reactor temperature

Figure 5. Conversion vs time curves for (a) reduction and (b) oxidation reactions for fresh and used particles. Reduction in N_2 and oxidation in air at 1000 ºC in TGA.

Figure 6. SEM images of fresh (right) and used (left) particles after 10 h in CLOU unit: (a, c) image of the particles; (b, d) image and EDX line profile of Cu (—), Ca (---), K (-··-), P (-·-), and Na (···) in a cross section of a particle.

Fig. 7. Experimental fractional conversion rate of char different fuels as a function of fuel reactor temperature: Biomass in CLOU process (--●--). Biomass in iG-CLC process (--○--) [29], Lignite (--▼--) [26], MV Bituminous (--▲--) [26], LV Bituminous (--■--) [26], and Anthracite (--♦--) [26].

Fig. 8. Carbon capture efficiency as a function of the fuel reactor inventory for biomass at two different temperatures in the fuel reactor: 900ºC(—), 920ºC (---).η_{CSS}=0; ϕ = 1.1.

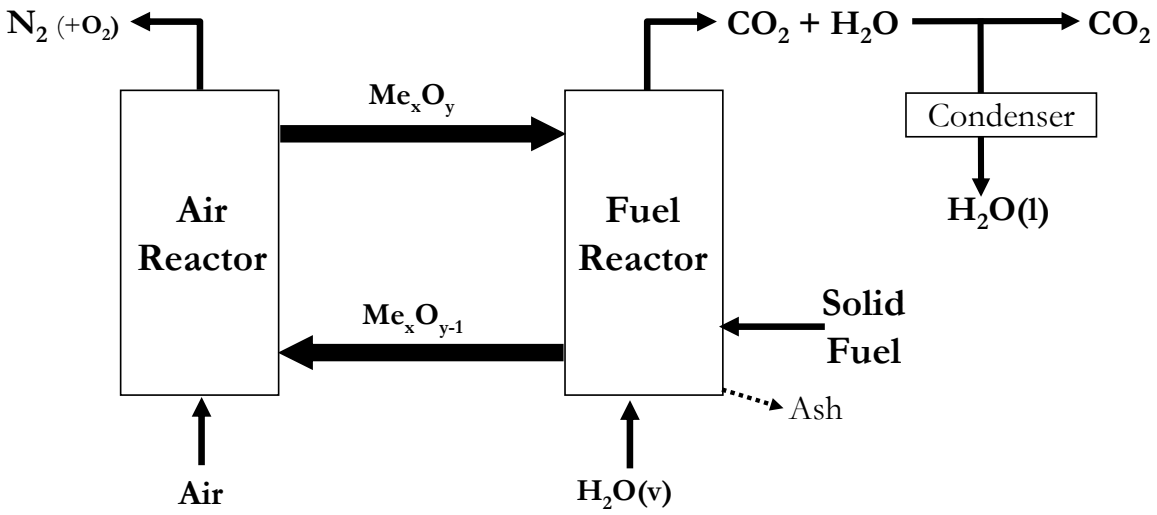

Fig. 1. Schematic layout of the CLOU system.

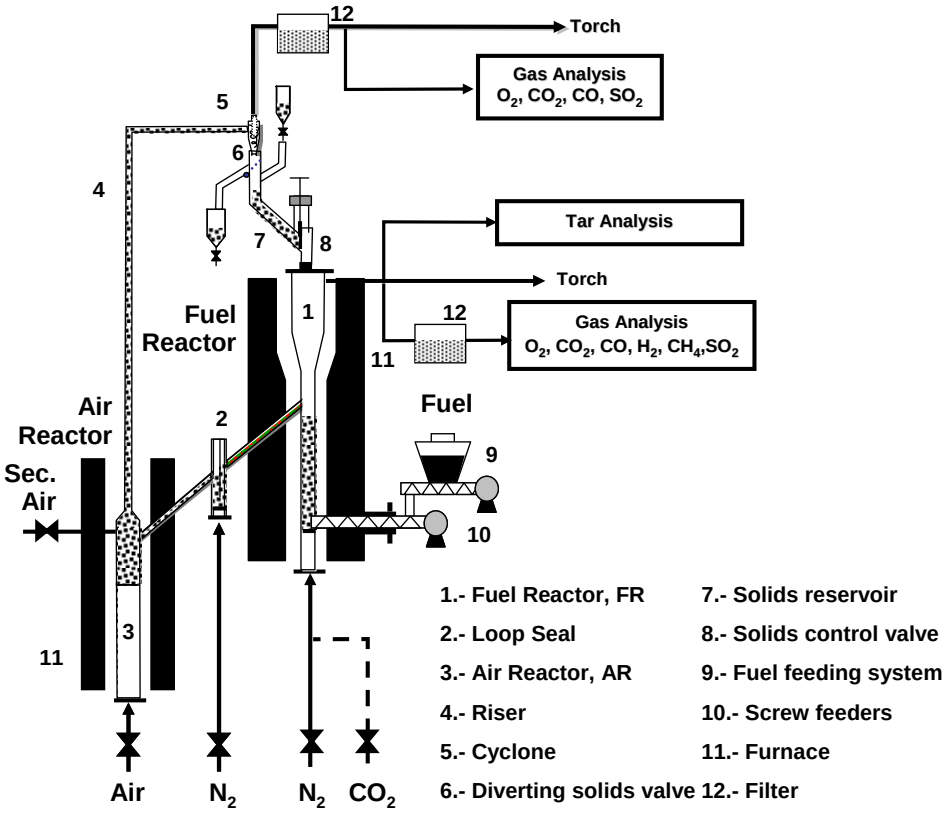

Fig. 2. Schematic view of the ICB-CSIC-s1 unit for the CLOU process (1.5 kW_{th}).

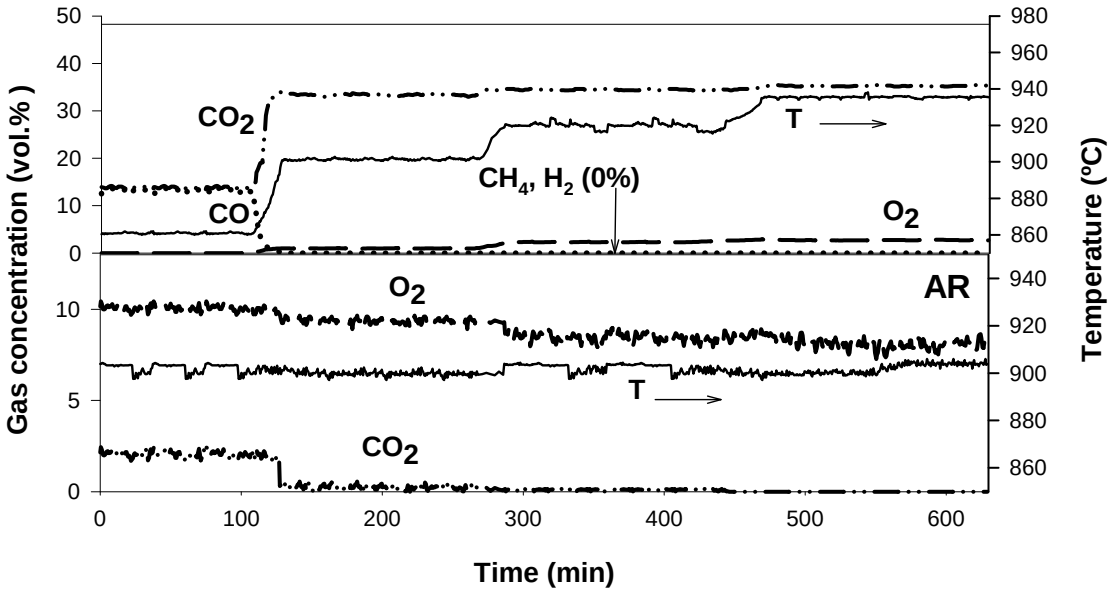

Fig. 3. Evolution of the gas composition in the air and fuel reactors as temperature in the fuel reactor was varied. $\dot{m}_{SF} = 0.24\ kg/h$.

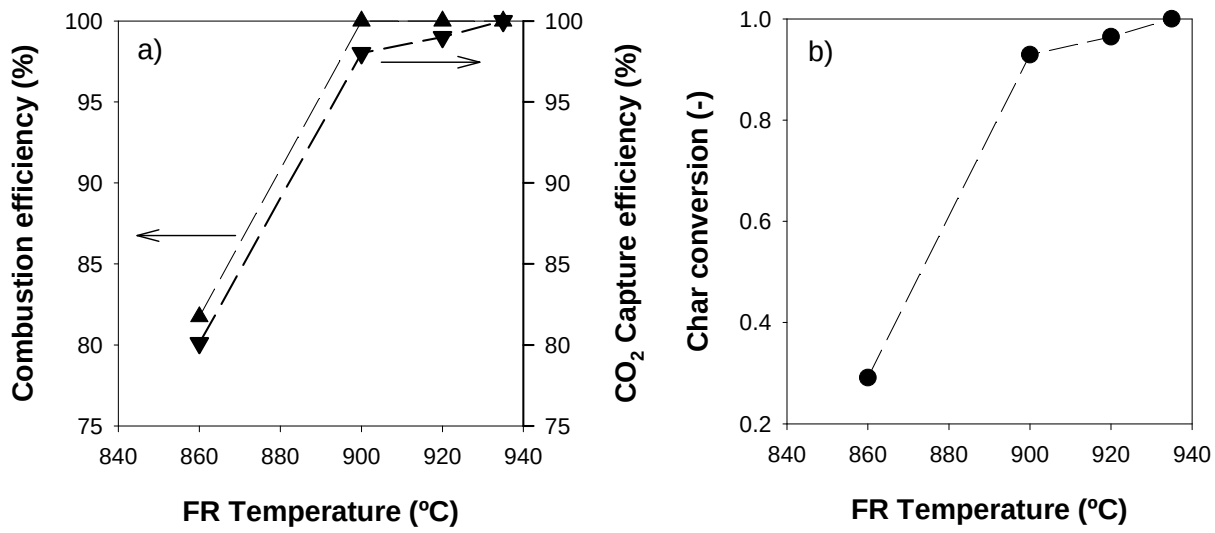

Fig. 4. (a) Combustion efficiency in the fuel reactor and CO_2 capture efficiency and (b) char conversion, as a function of the fuel reactor temperature

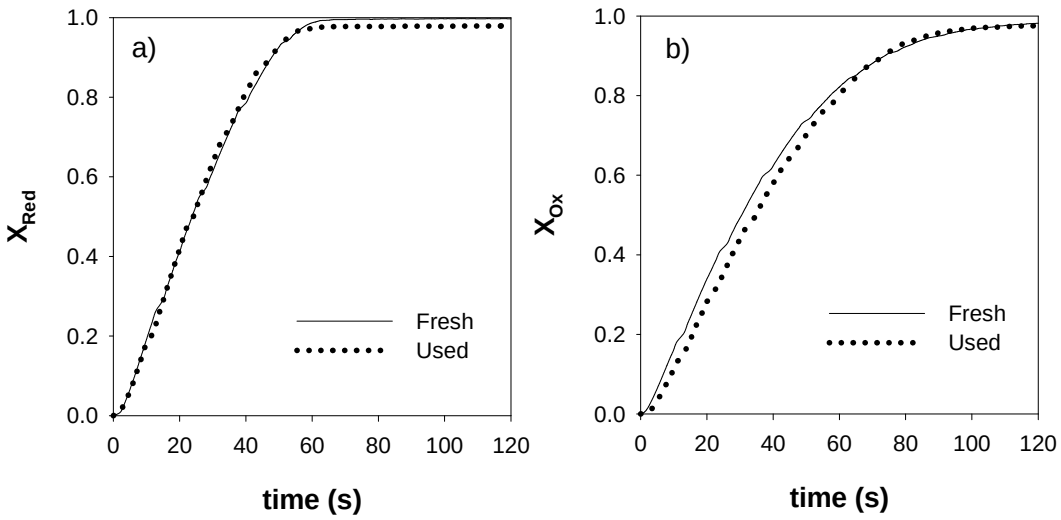

Figure 5. Conversion vs time curves for (a) reduction and (b) oxidation reactions for fresh and used particles. Reduction in N_2 and oxidation in air at 1000 ºC in TGA.

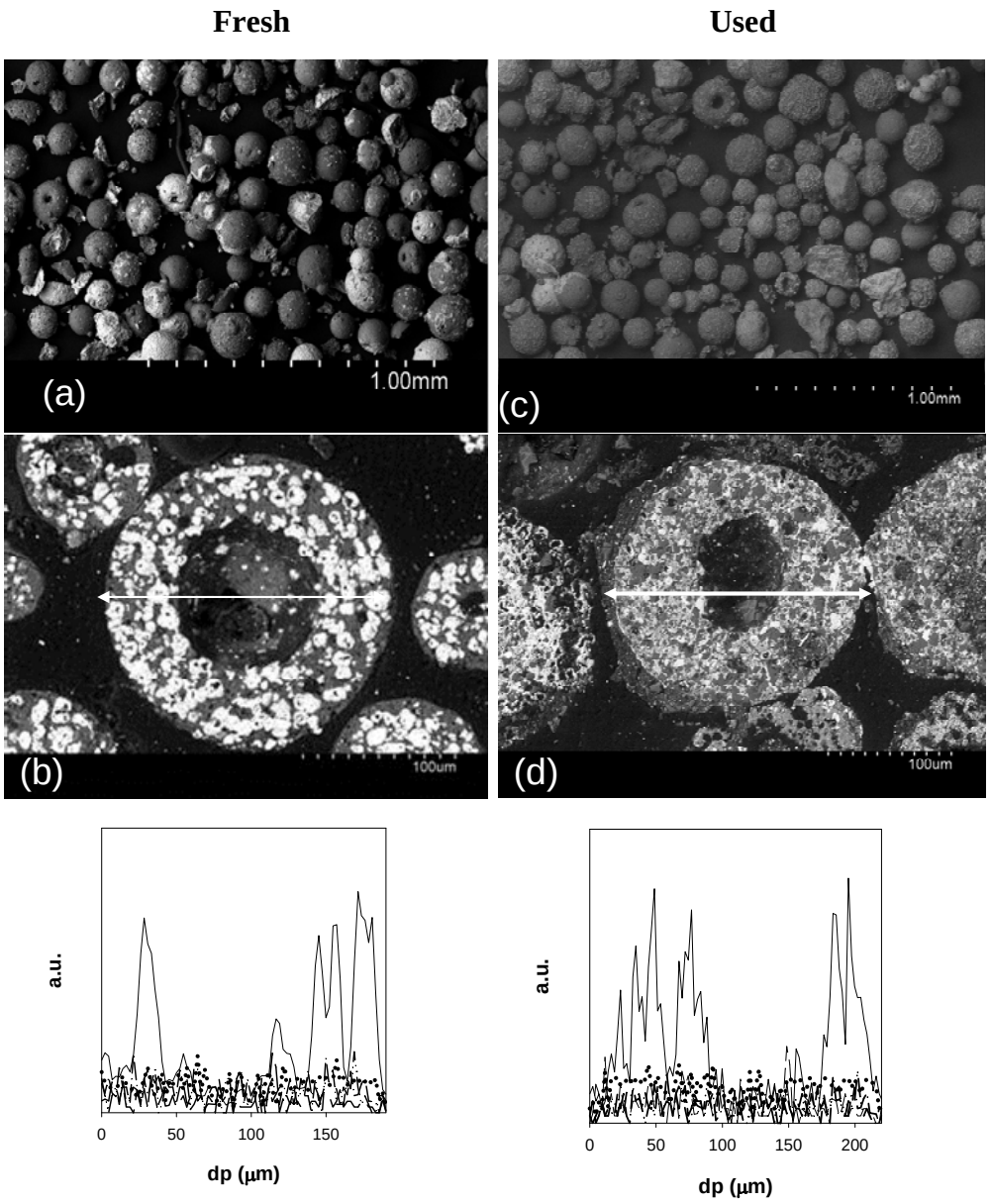

Figure 6. SEM images of fresh (right) and used (left) particles after 10 h in CLOU unit: (a, c) image of the particles; (b, d) image and EDX line profile of Cu (—), Ca (---), K (-··-), P (-·-), and Na (···) in a cross section of a particle.

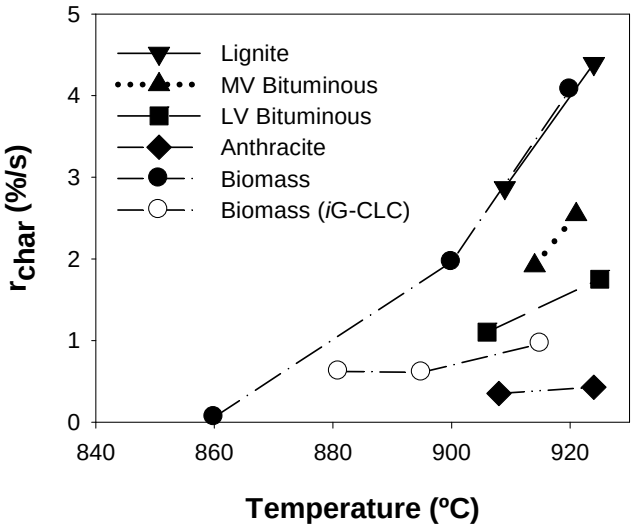

Fig. 7. Experimental fractional conversion rate of char different fuels as a function of fuel reactor temperature: Biomass in CLOU process (--●--). Biomass in iG-CLC process (--○--) [29], Lignite (--▼--) [26], MV Bituminous (--▲--) [26], LV Bituminous (--■--) [26], and Anthracite (--♦--) [26].

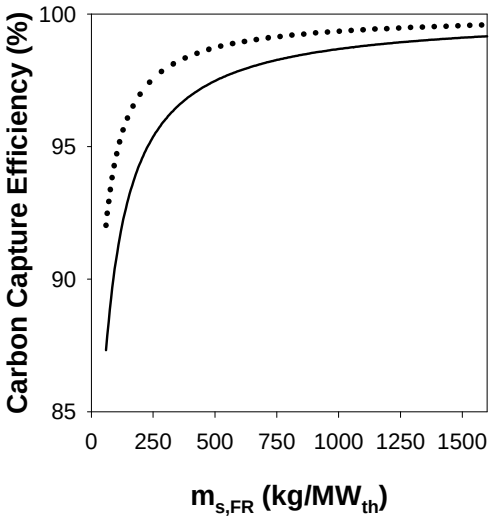

Fig. 8. Carbon capture efficiency as a function of the fuel reactor inventory for biomass at two different temperatures in the fuel reactor: 900ºC(—), 920ºC (---). η_{CSS}=0; ϕ = 1.1.